DEVELOPMENT OF PARTICLE BREAKDOWN AND ALUMINA STRENGTH DURING CALCINATION

Wind S, Jensen-Holm C and Raahauge B

F.L.Smidth A/S Minerals Denmark
Vigerslev Allé 77, DK-2500, Denmark

Abstract

Since the replacement of rotary kilns with stationary calciners, the impact from hydrate properties and calcination technology on the quality of Smelter Grade Alumina (SGA) have been studied frequently. F.L. Smidth is studying the complex interaction between calcining conditions, particle breakdown and development of alumina particle strength in both Pilot-scale and industrial calcination units using conventional analytical techniques. The pilot-scale units is simulating the pre-calcination step at 320-380°C, common to all stationary calciners and the final calcination stage at 1070°C in Gas Suspension Calciners without Holding Vessel. The calcining capacity of the full scale units are ranging from 2200-4500 TPD of SGA and cover stationary calciners with and without Holding Vessel. Representative hydrate samples from eight (8) different alumina refineries are flash calcined and compared. The first results of the above work will be presented with focus on how the calcining conditions impacts the properties of calcined industrial hydrates with respect to alumina strength and particle breakdown.

1. Introduction

Since the development of the F.L.Smidth Gas Suspension Calciner (GSC) for alumina was initiated back in 1976, the complex interaction between calcining conditions, particle breakdown and development of alumina particle strength in both pilot-scale and later industrial calcination units have been studied. The results of the first pilot-scale study was reported as early as 1982 [1,2] before the first 1000 TPD GSC unit was commissioned at Hindalco, India, in 1986 [3].

At that point in time relatively few stationary calciners were in operation and the major share of world alumina was still produced in rotary kilns. Consequently, the precipitation circuit in very few refineries was designed for producing a hydrate with sufficient strength to withstand the change in calcining conditions from rotary kilns to stationary calciners with respect to particle breakdown.

As time has passed, more and more rotary kilns have been replaced with stationary calciners [4], while new refineries was equipped with stationary calciners, with a few exceptions only [5]. Simultaneously, more [6] and more hydrate precipitation circuits were modified and optimized for producing a hydrate suitable for stationary calciners.

In view of the above development, and the fact that there is still a lot to learn and understand FLS and Alcoa decided to initiate a new hydrate calcination study in 2005 involving eight different alumina refineries equipped with FLS or Alcoa stationary calciners. In doing so, the major objectives were to study and understand the factors responsible for particle breakdown and development of alumina particle strength.

2. Gas Suspension Calciner Process Flow Sheet

FLS Gas Suspension Calciner comprises four main sections:

- Drying and Pre-heating/Pre-Calcination (PO1,PO2) of Feed material to Calcination Furnace (PO4);
- Calcination Furnace (P04) and Furnace Cyclone (P03) with/ without Holding Vessel (HVO3);
- Direct Heat Recovery from alumina by cooling with Air in Four (4) stage Cyclone cooler;
- Indirect alumina cooling with water in a Fluidized Bed Cooler.

The Drying and Pre-Heating/Pre-Calcination of Hydrate (PO1 & PO2 in Figure 1a) comprise two stages that are very similar in all calcination flow sheets and dictated by the drying requirement of moist hydrate with typically 6 – 9% moisture and the thermo chemistry of the calcination process.

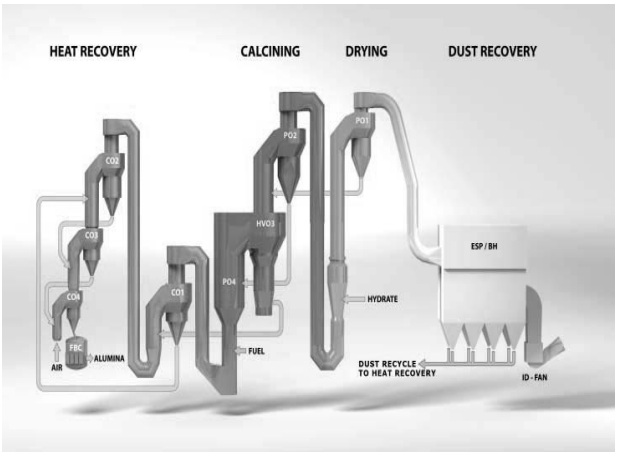

Figure 1a: FLS Gas Suspension Calciner (GSC) flow sheet.

Figure 1b: 3 x 4500 TPD GSC Units, QAL.

In the FLS and Alcoa calciner flow sheets, dust from drying cyclone (PO1) enters an ESP [4] or Bag House [4], from where it can be either fully or partially recycled back to the calcination process (dust management). The dust collected from the ESP or Bag House contains both gibbsite and a relatively high fraction of α-alumina phase as pointed out elsewhere [23].

3. Thermo Chemical Reactions – Simplified Reality

With the availability of more and more advanced solid state analytical methods [7,8] the dehydration pathway from gibbsite to α-alumina phase as well as the development of SGA microstructure and properties during calcination have received considerable interest lately [7,8,9,10]. However, with one exception [10], all of these investigations use laboratory scale calcining techniques which do not correctly simulate the flash calcining conditions prevailing in all industrial size stationary calciners with respect to fluid dynamic conditions and heating rates as closely as to be reported in this study. Unfortunately, some of these studies [7,8,19,20] has presented lot of speculation and thus created more confusion than real new information, especially about the impact of different calcination technologies on SGA properties.

The simplified thermo chemical reactions from alumina hydrate to smelter grade alumina in a GSC may be shown as:

Pre - calcination (P01-P02):

– 380°C

(1) Al_2O_3, $3H_2O$ + Heat => Al_2O_3, xH_2O + $(3 – x)H_2O$

Calcination (P04-P03/HVO3):

380 – 1075/940 °C

(2) Al_2O_3, xH_2O + Heat => i-Al_2O_3 + Al_2O_3 $(x–y)H_2O$ + yH_2O

Alpha alumina formation (P04-PO3/HV03):

1075/940°C

i-Al_2O_3 => α-Al_2O_3 + Heat

In the above endothermic reactions (1) and (2), the calcination reactions release water by the rate of heat-transfer to the reaction front in the solid particles. The final reaction (3) is the exothermal formation of α–alumina phase from mainly Rho-alumina (11) and some Boehmite phase (3-5%), through several intermediate steps of crystalline phase changes (Gibbsite => ρ => χ => γ' => δ => θ => α), in parallel with formation of significant amounts of X-ray amorphous phases. The formation of the X-ray amorphous phases dring flash calcination are according to Yamada (11) the reason for α–alumina phase formation at lower activation energies than through crystalline phase changes only.

The physical properties of the alumina changes with the dehydration as indicated in **Figure 2a** below.

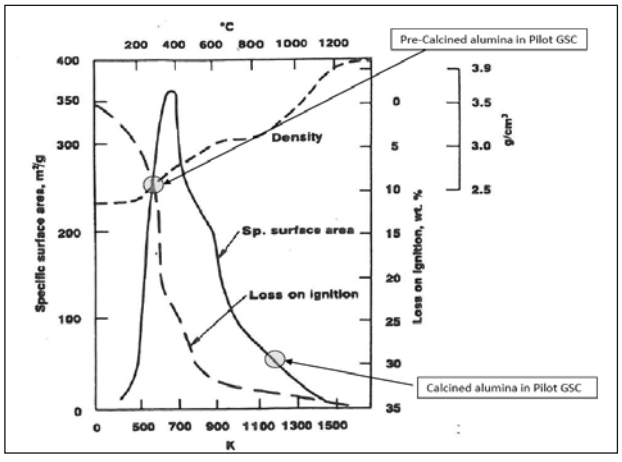

Figure 2a. Gibbsite Dehydration [Alcoa]

Figure 2b. Pilot-scale GSC test rig.

4. Hydrate and Alumina Test Materials

Representative alumina and hydrate samples from eight (8) different alumina refineries were included in the R&D program. Thin section microscopy has been used to determine and quantify the internal particle structure of the hydrates as Mosaic, Radial, and Pseudo-Radial structures [1,2].

The Mosaic particle structure is obtained mainly by agglomeration of many small seed hydrate particles in the precipitation circuit to produce a particle with a high concentration of grain boundaries. The Radial particle structure is obtained by agglomeration of a few seed hydrate particles followed by crystal growth to reach the final particle size with a low concentration of grain boundaries. The Pseudo-Radial particle structure is obtained by agglomeration of small seed hydrate particles followed by crystal growth to cement the agglomerated particles together to obtain a medium concentration of grain boundaries. In quantitative terms, Radial + Pseudo-Radial structure is referred to below as Non-Mosaic Structure (NMS).

5. Simulation of Industrial Size Calciner

The Pilot-scale GSC unit shown in Figure 2b simulates the pre-calcination processes between hydrate feed point and inlet to Calcination Furnace (Figure 1 & 2a) and the complete calcination process in one stage (Figure 12a).

The specific surface area (SSA) obtained at pre-calcination in the Pilot-GSC, is seen in Figure 2a, to have a peak value (240-245 m2/g) like the SSA indicated in Figure 3a below. In full scale calciners, the SSA in the feed material to the Calciner Furnace is somewhat lower (150-180 m2/g) owing to slightly different temperature and internal fines circulation caused by cyclones having less than 100% collection efficiency. The pre-calcined samples contained Gibbsite and about 5% Boehmite plus a large fraction of X-Ray amorphous material, all in line with expectations and previous findings in pilot plant and industrial calciners [2,11]. The SSA of the fully calcined hydrate in Figure 3a is seen to correspond to the SSA in full scale calciners as shown for hydrates from Plant G (72-73 m2/g) and Plant B (68-69 m2/g) respectively. Neither Gibbsite nor Boehmite phase was detected in alumina from the Pilot GSC and Plant samples proving that complete calcination to SGA has taken place.

With respect to the α-phase formation in the Pilot GSC, this was about 0 – 30% owing to the distributed gas burner heating needed to maintain the temperature profile.

In general, the same alumina phases are detected by XRD in the Pilot GSC and Plant calcined samples. It is therefore concluded that the Pilot GSC is able to simulate Plant calciners with respect to degree of calcination (LOI & SSA). However, with the heating rate in the Pilot GSC somewhat higher than in Plant calciners because the complete calcination process is performed in one single stage only.

A modified Forsythe-Hertwig Attrition Index (AI) test has been used to measure the particle strength of hydrates and alumina.

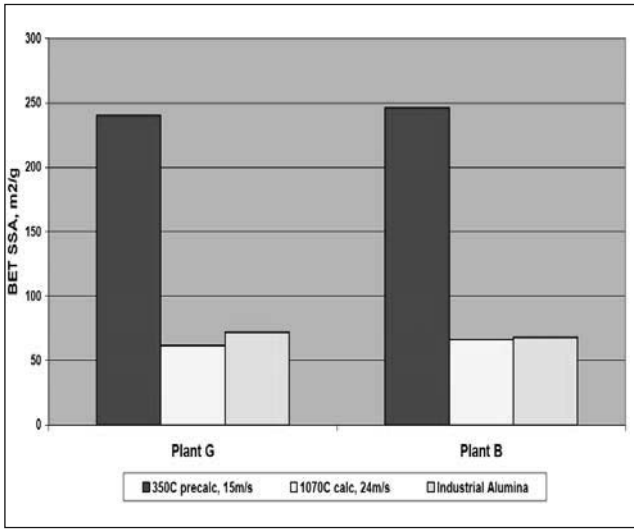

Figure 3a: SSA (BET) GSC Pilot & Plants

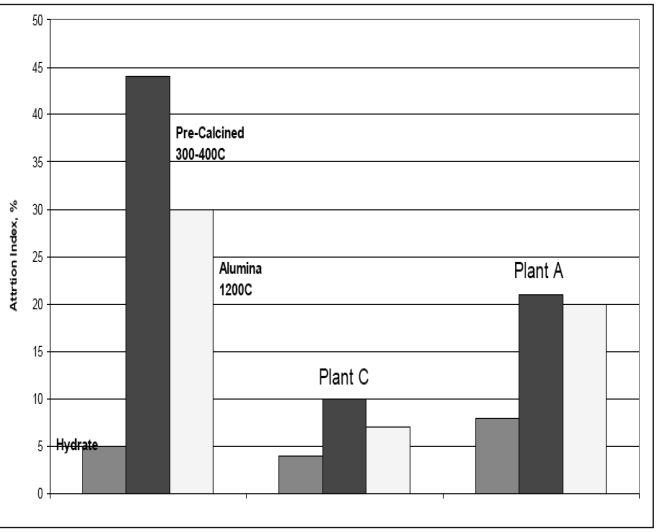

Figure 3b: Attrition Index GSC Pilot & Plants

6. Development of Alumina Particle Strength

This material strength test is well known in the alumina industry. The higher the AI value the weaker is the hydrate or alumina particles tested. As seen in **Figure 3b** for the Radial (Left), Mosaic (Plant C) and Pseudo-Radial (Plant A) hydrates tested, the AI of pre-calcined alumina phase formed at 300-400°C as per reaction (1) above, is measured to be much weaker (higher AI) than its corresponding hydrate. However, the alumina may regain some of its particle strength (lower AI than pre-calcined alumina) during final calcination in accordance with reaction (2) above as new crystalline and amorphous solid-state phase-change reactions takes place forming new and stronger chemical bonds.

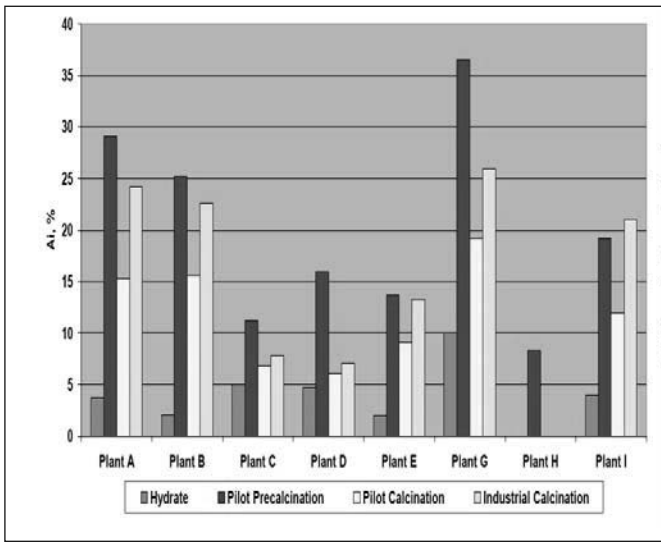

Figure 4a: Attrition Index versus Degree of Calcination.

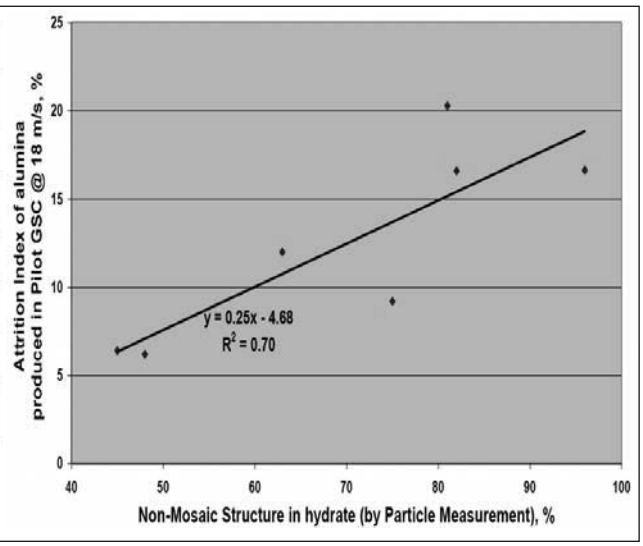

Figure 4b: Alumina Attrition Index versus Particle Structure.

The attrition index test is a very rough test with respect to the fluid dynamic conditions when compared to Plant calciners and focuses on one cut point (45µm) only of the entire particle size distribution. Anyway, the modified Forsythe-Hertwig Attrition Index test today is a standard in the alumina industry. It has been used by Sang [14], to correlate particle breakdown in Fluid-Flash calciners with Attrition Index of calcined hydrate in the laboratory ($R^2 = 0.96$).

The measured increase in Attrition Index, or "weakness", at low temperature of the pre-calcined hydrate seen in **Figure 3b**, is also observed in Plant GSC units in the pre-calcined material fed to the Calciner Furnace. These observations contradicts the findings of Klett et all [17] based on hydrate samples calcined in a muffle furnace.

The alumina from Plant calcination units in **Figure 4a** are measured to be weaker (higher AI) than alumina from the Pilot GSC unit, but this is mainly due to the higher heating rate during Pilot GSC calcination - and not due to the observed particle breakdown. Earlier bench-scale investigations by Zwicker [12] have concluded that a high heating rate produces a relatively stronger particle with lower AI.

This has previously been reported by FL Smidth [18], comparing AI of the alumina from a rotary kiln equal to 18% (14% α-phase) with AI of the alumina from a Gas Suspension Calciner equal to 14% (3% α-phase) using the same hydrate and having the same particle breakdown of 2%. However, other factors than the heating rate, is responsible for obtaining a strong alumina particle after calcinations, i.e. hydrate soda content and structure of the hydrate [21]. This is seen in **Figure 4b** above, where the weakness of the alumina particle as measured by the AI, increases with increasing content of Non-Mosaic particle structure ($R^2 = 0.70$).

7. Particle Size Distribution (PSD) and Particle Breakdown during Calcination

When hydrate is calcined in the Pilot GSC at different gas velocities, the PSD of the hydrate changes as a result of particle breakdown, taken place during calcination.

Particle breakdown during calcinations is calculated from the amount of fines (< 45 microns) and super fines (< 20 micron) before and after calcination from material samples and analysis (< 45 micron on Rotap Sieve and < 20 micron by Malvern laser diffractometry):

$PB(45\ \mu m) = X_{Alumina} - X_{Hydrate}$

$PB(20\ \mu m) = Y_{Alumina} - Y_{Hydrate}$

Where: X_i:= wt-% < 45µm of hydrate or alumina measured by Rotap Sieve;

Y_i:= % < 20µm of hydrate or alumina measured by Malvern Laser PSD;

To reduce impact on uncertainties on the mass balances during the calcinations tests, a simple but stable method is used by comparing the fine fraction sizes of hydrate feed and calcined hydrate. This calculation neglects the insignificant amount of dust overflowing from the test cyclone, verified by the 2 – 5 micron range cut-size (particle size of which 50% is collected) of the cyclone, introducing only a very small error.

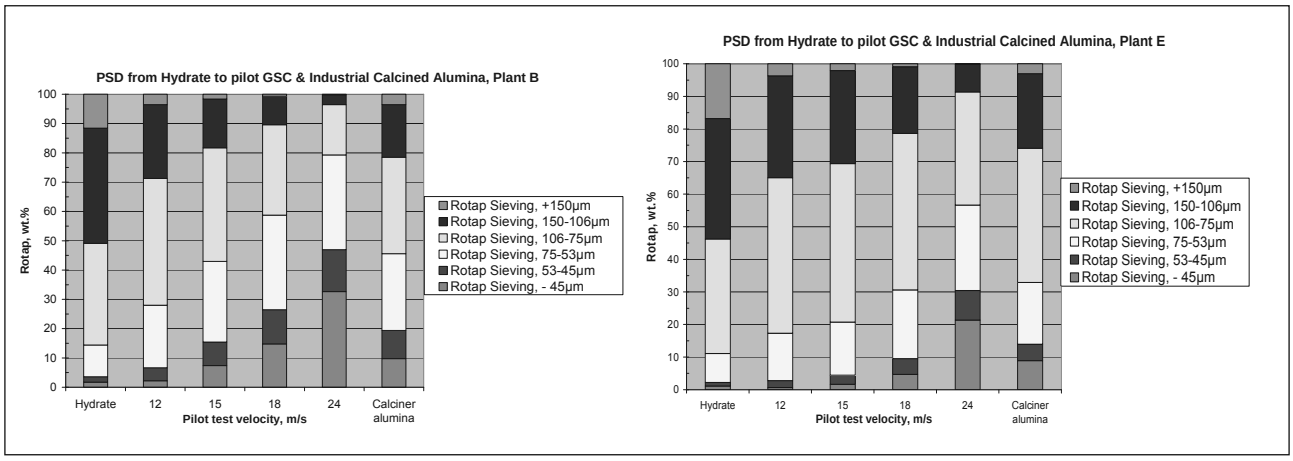

Figure 5a. Hydrate and Alumina from Plant B.

Figure 5b. Hydrate and Alumina from Plant E.

In the above **Figure 5a** it can be seen that if the Pilot GSC is operated at a gas velocity between 15 -18 m/sec, then the same amount of alumina below the 45 micron particle size will be generated as from a Plant Calciner, shown in the column to the very right in **Figure 5a**.

It is therefore reasonable to conclude that the Pilot GSC is representative with respect to simulating the fluid dynamic condition in Plant calciners. Comparing the change of PSD of Plant B (**Figure 5a**) during calcination with the PSD of Plant E hydrate (**Figure 5b**), it can be deducted that Plant E hydrate is more resistant to particle breakdown than Plant B hydrate, because Plant E hydrate can be calcined at 18-24 m/sec in order to breakdown down the same amount as Plant B hydrate calcined at 15-18 m/sec. However, the + 150 micron particle size fractions of both Plant B hydrate and Plant E hydrate are almost equally sensitive to particle breakdown in the 12 – 15 m/sec test velocity range.

In general considering the changes in PSD from hydrate to alumina, it is possible to identify whether particle size has an influence on the particle breakdown. It can be seen and concluded that a main contributor of particle breakdown is related to the fraction of coarse hydrate particles (+106µm). The coarse particles are exposed to relative higher centrifugal force on the wall (and have higher kinetic energy) compared to smaller particles of the same velocity which lead to higher particle breakdown.

8. Particle Breakdown Models

The first generation particle breakdown model developed by FLS was solely based on pilot plant testing in 1980 – 81 [2] and included the below parameters:

a) Solid Sodium Oxalate occluded in the hydrate particles
b) Quantity of Non – Mosaic Particle Structure
c) Attrition Index of the Hydrate and Calcined Alumina
d) Hydrate particle size distribution

However, recent particle breakdown data from Plant GSC units on different refinery hydrates showed that the first generation model was not fully adequate any more and consequently a revised model was to be developed.

8.1 The Centrifugal Acceleration Model

When a particle passes the curved riser duct and cyclones (see **Figure 6a**) in the calcination plant, the centrifugal acceleration acting on the particles caused by the swirling gas flow, forces the particles against the wall of the riser ducts and cyclones. The centrifugal forces acting on the particles when they pass a riser duct or cyclone with a characteristic radius of curvature of R at a tangential velocity of U_t is:

PB $\propto$ Centrifugal Force on particle = $m_p * U_t^2 / R \propto dp^3 * U_t^2$

Where:

m_p = Particle mass $\propto \rho_{particle} * dp^3$

ρ_p = Particle density

dp = Particle diameter

U_t = Tangential velocity (eg cyclone inlet gas velocity)

R = Radius of curvature (eg cyclone radius)

From the above relation one would expect that particle breakdown will increase with:

Increasing particle size due to the increased kinetic energy of the particle as observed above, and;

The gas velocity into the riser ducts and the cyclones raised to the 2nd power;

This suggests a simple 2nd Order Power Law Model with respect to gas velocity. Other physical considerations results in a similar dependency of particle breakdown on gas velocity.

8.2 The Gas Impulse Model [16]

Saatci et all shows in their work [16], that the increase in the fraction < 45 micron of hydrate calcined in a muffle furnace at 1000°C, increases linearly with the impulse (kg m/sec) of the gas/air in the orifice of the Forsythe-Hertwig Attrition Index test apparatus ($R^2 = 0.82$). From dimensional analysis, the Gas Impulse Model can be expressed and interpreted as below:

Gas Impulse (kg m/sec) = $v_G w_G = v_G G \theta_{Batch} = v_G G \theta_{Continous} = v_G v_G \rho_G A_o \theta_{Continous} = v_G^2 \rho_G A_o \theta_{Continous}$

Where,

v_G (m/sec) = gas/air velocity in the orifice;

w_G (kg) = mass of gas/air passing through Attrition Test orifice during the test period;

G (kg/sec) = mass flow of gas/air in the orifice;

θ_{Batch} (sec) = duration of Attrition Test period;

$\theta_{Continous}$ (sec) = Retention time of solids in continuously operating calciners;

ρ_G (kg/m^3) = Gas/air density

A_o (m^2) = Open area of orifice;

Saatci et all conclude that the gas/air jet strain in commercial calciners is most likely the most relevant fluid dynamic factor for particle breakage during calcination. However, the above analysis suggests that also the average retention time must be factored in to the gas impulse parameter.

In addition to the above commonality between the models (6 & 7) with respect to the gas velocity, the Gas Impulse Model [16] also includes the retention time of solids which is about 30 minutes in Circulating Fluid Bed calciners [17]. Furthermore, the Circulating Fluid Bed reactor operates at relatively high fluidization velocities [22] compared to classical fluid beds such as Fluid bed coolers and Holding vessels where relatively low fluidization velocities do not contribute to the particle breakdown [17].

8.3 The Cyclone Attrition Rate Model [24]

Wherther and Thon [24] has presented the below specific attrition rate model for cyclones, which shows reasonable correlation with their experimental results on a vanadium penta oxide catalyst:

$(1/M_{in})\, dw/dt = C_c * d_p * U_t^2 * \mu^{-0.5}$

Where : M_{in} = mass flow rate of solids in to the cyclone (kg solid/sec);

w = mass of particles breaking down by attrition below a certain size, i.e. 45 micron;

t = time in seconds;

C_c = material and equipment constant with respect to reistance towards particle attrition/breakage;

$\mu = (M_{in} / G_{in})$ mass-loading, (i.e. the solid to gas mass-flow ratio in to the test cyclone;

G_{in} = mass flow of gas in to the cyclone (kg gas/sec);

According to Whether and Thon, a relatively high mass-loading may generate a "cushion" effect because the probability of an individual particle to collide with the wall decreases in a single-pass cyclone. However, the "cushion" effect may disappear in a multi-pass cyclone as new particles are exposed to wall collisions at every new pass before leaving the reactor system such as in a Circulating Fluid Bed (CFB) reactor [17].

While the introduction of the mass-loading into the rate model makes sence in general, it is not taking the size of the cyclone into consideration, making scale-up considerations more difficult. Doing that we find:

$(1/M_{in})\, dw/dt = C'_c * d_p * (U_t^2/R) * \mu^{-0.5}$

C'_c is now a true material constant with respect to resistance towards particle attrition/breakage. Integrating equation (8) we find the average particle attrtion/breakdown rate in the cyclone to be:

$\Delta w / \Delta t = C'_c * d_p * (U_t^2/R) * (M_{in} * G_{in})^{0.5}$

It is now evident that a high mass-flow into the cyclone, being single- or multi-pass increases the average rate of particle attrition/breakdown according to the above model. Taking the analysis above one step further substituting $G_{in} \propto U_t$ we find:

$\Delta w / \Delta t = C'_c * d_p * (U_t^2/R) * \mu^{0.5} * G_{in} \propto C'_c * d_p * \mu^{0.5} * U_t^3$

Now we see that the average attrtion rate in the cyclone increases with the mass-loading in to the cyclone and the gas velocity raised to the 3rd power.

8.4 Particle Breakdown Model Summary

Summarizing, all the above particle attrition/breakdown models, the particle breakdown (PB) is as a first approximation described by the following power law equation, assuming constant mass-loading and particle size:

$PB(U) = \beta + \alpha U2$

Where: U = Characteristic gas velocity – cyclone gas inlet velocity used in this work, or orifice gas/air velocity in the Saatci et all work [16]. α = Velocity rate factor for particle breakdown for a specific hydrate at constant particle size, plant design and mass-loading.

β = Characteristic constant, specific for hydrate used to model pilot test results and including other factors than gas velocity.

9. Particle Breakdown Observation from Pilot Test Calcination

The calcination test results at 1075°C in Figure 6b, shows that the particle breakdown for each individual hydrate tested is a linear function with respect to the cyclone inlet gas velocity raised to the 2nd power (U2) for the gas velocity range studied, R2 = 0.77 - 1.00. As can be observed, all β values is < 0, i.e zero (0) wt.% particle breakdown at about U2=150m2/s2, i.e., at a cyclone inlet gas velocity of about 12 m/s.

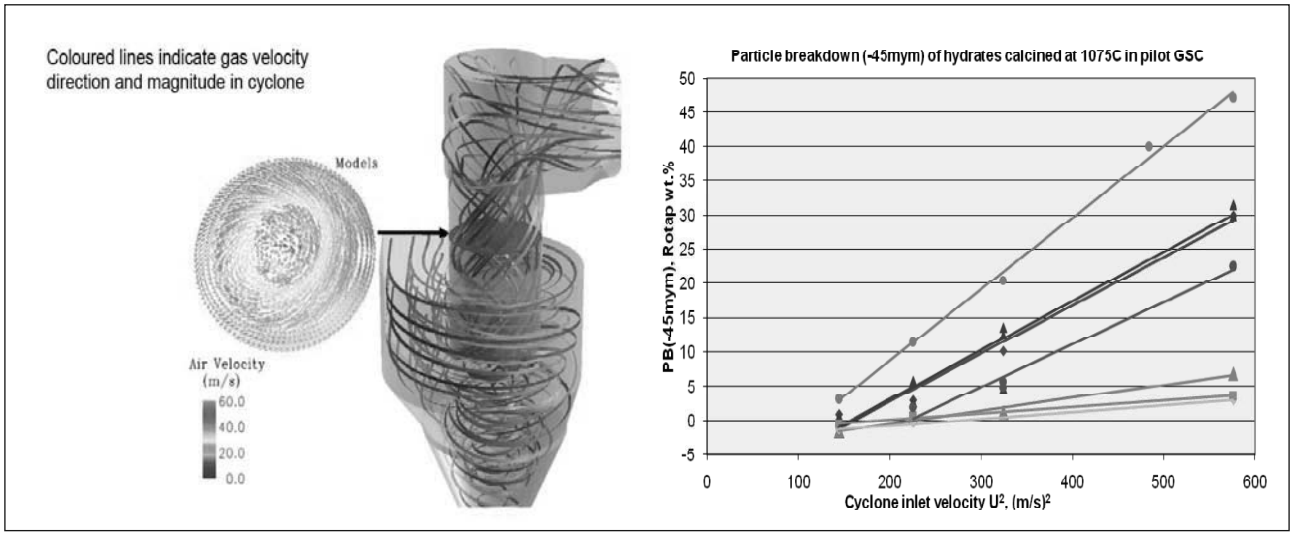

Figure 6a. CFD Model of Cyclone

Figure 6b. Calcination Particle Breakdown - 1075°C

The experimental fact that no particle breakdown can be measured at a cyclone inlet gas velocity of about 12 m/sec and lower, suggests the following conclusions:

Particle shrinkage reported by Klett et all [17] has no practical impact on particle breakdown.

The theory of steam explosion caused by Boehmite phase proposed by Peander et all [8] has no practical impact on particle breakdown either.

The particle breakdown in a Plant GSC is typical about 30-40% of the particle breakdown in a Pilot GSC, when operating at the same gas velocity, which is due to the net effect of different size, equation (6), and geometry of the cyclones, as well as a much lower mass-loading in the Pilot GSC than in the Plant GSC units.

In **Figure 7a** below, the particle breakdown data from the 1075°C calcination test of all the hydrates is plotted versus the attrition index of all the alumina products collected from the test.

Though a certain trend can be observed in **Figure 7a (**$R^2 = 0.33$), there is no simple correlation between the particle breakdown and alumina Attrition Index [13] in general.

Now, defining a new independent parameter $X = AI_{Alumina} \times U^2$ we find the empirical curve fit in **Figure 7b** with $R^2 = 0.9837$ covering particle breakdown of all hydrates tested at 12 – 24 m/sec gas velocity in to the cyclone:

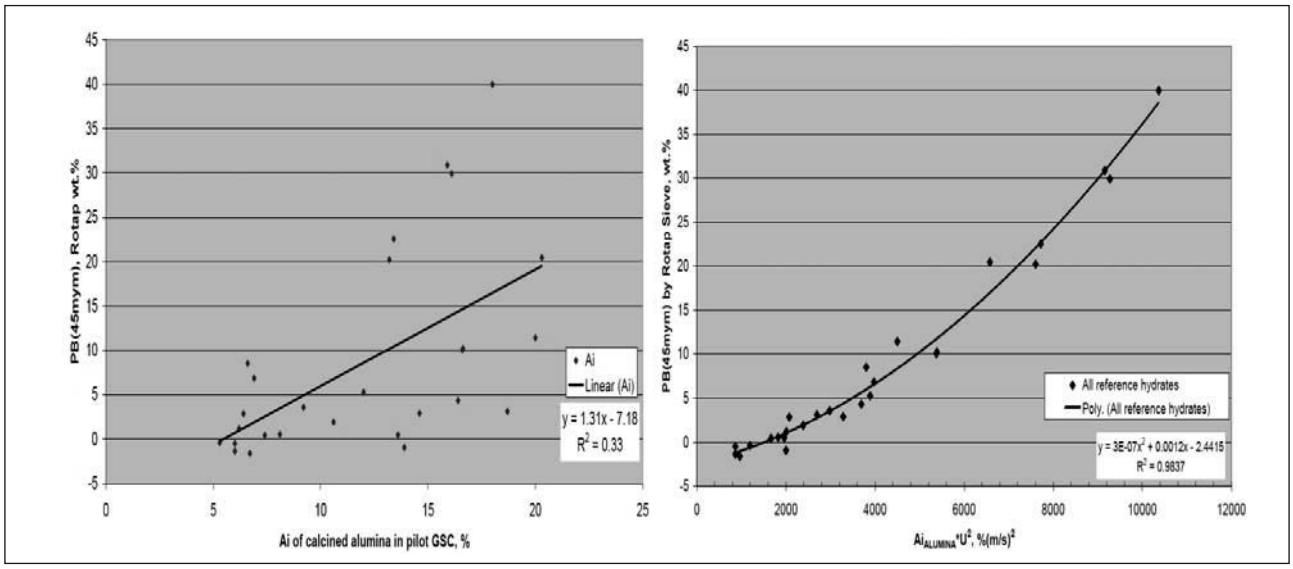

Figure 7a. Particle Breakdown vs Alumina AI

Figure 7b. Generic Particle Breakdown Model

Based on the alumina hydrate strength R&D project reported here, a new Generic Particle Breakdown Model for the Pilot GSC calcination test unit have been discovered by FLSmidth.

The Generic Particle Breakdown Model has been established on eight (8) reference hydrates from different alumina refineries and precipitation technologies. The Generic Particle Breakdown Model is based on a material property parameter (attrition index of calcined alumina) and a GSC design parameter (cyclone gas inlet velocity):

$PB(45\mu m) = 2.7\times10^{-7}\times X^2 + 1.2\times10^{-3}\times X - 2.4$ wt-%

Where: $X = AI_{Alumina}\times U^2$

$AI_{Alumina}$ = Attrition index of calcined alumina from Pilot GSC test, wt- %;

U = Pilot cyclone inlet gas velocity, 12 – 24 m/s;

Again, particle breakdown becomes zero (0) wt-% for U < 10 m/sec at an Alumina Attrition Index of 15wt-%, confirming the conclusions based on the single hydrate particle breakdown model in equation (13) above.

Since it has been demonstrated that the Pilot GSC is representative for the fluid dynamic conditions in an Plant calciner, there are strong indications that the Generic Particle Breakdown Model also applies to Plant calciners.

10. Conclusions and Recommendations

The above reported work suggests the following conclusions:

The Pilot GSC operation is representative for Plant calciner operation with respect to degree of calcination and fluid-dynamic conditions.

During pre-calcination minor amounts of Boehmite phase is formed, corresponding to the amount found in the material flow in to the Calciner furnace in Plant calciners, confirming the main gibbsite dehydration pathway through Rho-alumina and amorphous phases, already reported many years ago [11].

The observed particle breakdown is reduced to zero, when the gas velocity into the GSC Pilot cyclone is reduced to below about 9 - 12 m/sec, indicating that no measurable particle shrinkage takes place.

Despite higher heating rates in the GSC Pilot compared to Plant calciners, NO explosive shattering of the grains or particles takes place which is of practical significance. This confirms previous experimental findings that such a mechanism is not causing particle breakdown in Plant calciners either.

The observed particle breakdown at pre-calcination (360°C) and full calcination (1075°C) can be explained by a single parameter $X = AI_{Alumina}\times U^2$, including the Attrition Index of Alumina (particle weakness) and the gas velocity into the cyclone, squared.

Coarse particles (> 100 micron) are the main source of particles breaking down to less than 45 micron. This has been verified in Plant calciners as well.

Hydrate over-coarsening is therefor the wrong way to make alumina with maximum 10% < 45 micron because weaker alumina particle results, as previously reported [14].

In view of the above, Plant calciners can be designed with lower gas velocities to minimize particle breakdown, but this may not result in a strong alumina particle. Consequently, the real challenge is for the Alumina refiner to produce a hydrate which upon calcination becomes alumina with a low Attrition Index, so that a strong alumina particle is produced. This will minimize attrition or particle breakdown during calcination and transport from the calciner to the smelter, and subsequently when the alumina is used in the dry gas-scrubbing plant of the off gases in the smelter [15].

Needles to say this challenge points to the hydrate precipitation stage in the refinery, and the requirement for proper balancing of the many factors at play in precipitation of the hydrate. However, since a very coarse particle size distribution is not the answer a gain in yield may be achieved at the same time.

References

1. B.E. Raahauge,et al.: "Application of Gas Suspension Calciner in Relation to Bayer Hydrate Properties", The Australasian Institute of Mining and Metallurgy, 1981 Annual Conference, Sydney NSW, 1981.
2. B.E. Raahauge,et al.: "Energy Saving Production of Alumina with Gas Suspension Calciner", 111th AIME Annual Meeting, Dallas,US,1982.
3. T.A.Venugopalan,"Experience with Gas Suspension Calciner for Alumina", Proceedeings 1st International Alumina Quality Workshop, pp 53-66,(1988).
4. S.Wind and B.E.Raahauge: "Energy Efficiency in Gas Suspension Calciners (GSC)",TMS Light Metals, pp 235-240 (2009).
5. J.Ilkjaer, L.Bastue and B.E.Raahauge:"Alumina Calcination with the Multi Purpose Calcine", TMS Light Metals, pp 107-111, (1997).
6. O. Tsamper:"Improvements by the New Alusuisse Process for producing coarse Aluminium Hydrate in the Bayer Process", TMS Light Metals, pp 103-115(1981).
7. L.M.Perander et all,"Short- and long-range order in Smelter Grade Alumina – Development of Nano- and Microstructure during the Calcination of Bayer Gibbsite", TMS Light Metals, pp 29-35 (2008).
8. L.M.Perander et all," Impact of Calciner Technologies on Smelter Grade Alumina Microstructure and Properties" Proceedeings 8th International Alumina Quality Workshop, pp 103-107 (2008).
9. B. Wittington and D.Illevski, "Determination of the gibbsite dehydration reaction pathway at conditions relevant to Bayer refineries", Chemical Engineering Journal 98 (2004) pp 89-97.
10. V.J. Ingram-Jones et all,"Dehydroxylation sequences of gibbsite and boehmite study of differences between soak and flash calcination and particle size effects", J. Mater. Chem. 1996,6(1),73-79
11. K. Yamada, "Dehydration Products of Gibbsite by Rotary Kiln and Stationary Calciner" TMS Light Metals, pp 157-171, (1984).
12. J.D. Zwicker, "The Generation of Fines due to Heating of Aluminium Trihydrate", TMS Light Metals, pp 373-395 (1985).
13. P.Clerin and V.Laurent,"Alumina Particle Breakage in Attrition Test",TMS Light Metals, pp 41-47 (2001).
14. J.V. Sang:"Factors Affecting the Attrition Strength of Alumina Products",TMS Light Metals, pp 121-127,(1987).
15. Chandraskar, S. et all,"Alumina Fines' Journey from Cradle to Grave". Proceedings of the 7th International Alumina Quality Workshop, Perth, Australia (2005).
16. A.Saatci et all,"Attrition Behavior of Laboratory Calcined Alumina from Various Hydrates and its Influence on SG Alumina Quality and Calcination Design",TMS Light Metals, pp 81-86,(2004).
17. C.Klett et all,"Improvements of Product Quality in Circulating Fluidized Bed Calcination", TMS Light Metals, pp 33-38, (2010).

18. B.E. Raahaugel,"Experience with Gas Suspension Calciner for Alumina", TMS Light Metals, (1991).
19. L.M.Perander et all,"The Nature and Impacts of Fines in Smelter Grade Alumina", Journal Of Metals, pp.33-39,November 2009.
20. L.M.Perander, J.B.Metson and C.Klett,"Two Perspectives on the Evolution and Future of Alumina",TMS Light Metals, pp151-155,(2011).
21. L. Armstrong et all "Alumina Attrition – Investigation of Hydrate structure", Proceedings 4th International Alumina Quality Workshop, pp 239-249, Darwin, Australia (1996).
22. H-W. Schmidt, "Alumina Refinery Fundamentals – Theory and practice of Alumina Calcination – Circulating Fluid Bed (CFB) Perspective" Short Course TMS 2009.
23. G.J.Mills and B.E. Raahauge, "Developments in Calcination Technology for Smelter grade Alumina", Proceedings 6th International Alumina Quality Workshop, Brisbane, Australia.
24. A.Thon and J.Werther,"Attrtion resistance of a VPO catalyst", Applied Catalysis A: General 376 (2010) pp 56-65.